The potential significance of microbial Fe(III) reduction during deposition of Precambrian banded iron formations

K. O. KONHAUSER,[1] D. K. NEWMAN[2] AND A. KAPPLER[3]

[1]*Department of Earth and Atmospheric Sciences, University of Alberta, Edmonton, Alberta, Canada*
[2]*GPS Division, California Institute of Technology, Pasadena, California, USA*
[3]*Center for Applied Geoscience, University of Tübingen, Tübingen, Germany*

ABSTRACT

During deposition of late Archean–early Palaeoproterozoic Precambrian banded iron formations (BIFs) the downward flux of ferric hydroxide ($Fe(OH)_3$) and phytoplankton biomass should have facilitated microbial Fe(III) reduction. However, quantifying the significance of such a metabolic pathway in the Precambrian is extremely difficult, considering the post-depositional alteration of the rocks and the lack of ideal modern analogues. Consequently, we have very few constraints on the Fe cycle at that time, namely (i) the concentration of dissolved Fe(II) in the ocean waters; (ii) by what mechanisms Fe(II) was oxidized (chemical, photochemical or biological, the latter using either O_2 or light); (iii) where the ferric hydroxide was precipitated (over the shelf vs. open ocean); (iv) the amount of phytoplankton biomass, which relates to the nutrient status of the surface waters; (v) the relative importance of Fe(III) reduction vs. the other types of metabolic pathways utilized by sea floor microbial communities; and (vi) the proportion of primary vs. diagenetic Fe(II) in BIF. Furthermore, although estimates can be made regarding the quantity of reducing equivalents necessary to account for the diagenetic Fe(II) component in Fe-rich BIF layers, those same estimates do not offer any insights into the magnitude of Fe(III) actually generated within the water column, and hence, the efficiency of Fe and C recycling prior to burial. Accordingly, in this study, we have attempted to model the ancient Fe cycle, based simply on conservative experimental rates of photosynthetic Fe(II) oxidation in the euphotic zone. We estimate here that under ideal growth conditions, as much as 70% of the biologically formed Fe(III) could have been recycled back into the water column via fermentation and organic carbon oxidation coupled to microbial Fe(III) reduction. By comparing the potential amount of biomass generated phototrophically with the reducing equivalents required for Fe(III) reduction and magnetite formation, we also hypothesize that another anaerobic metabolic pathway might have been utilized in the surface sediment to oxidize the fermentation by-products. Based on the premise that the deep ocean waters were anoxic, this role could have been fulfilled by methanogens, and maybe even methanotrophs that employed Fe(III) reduction.

INTRODUCTION

Banded iron formations are chemical sedimentary rocks that were precipitated throughout much of the Late Archean and Palaeoproterozoic (2.7–1.9 Ga). They are characteristically laminated, with alternating Fe-rich and Si-rich layers (Table 1). Banding can be observed on a wide range of scales, from coarse macrobands (meters in thickness) to mesobands (centimeter-thick units) to millimeter and submillimeter layers (Trendall & Blockley, 1970). Among the latter is the wide variety of varve-like repetitive laminae, known as microbands.

Despite the absence of direct evidence, it is becoming increasingly accepted that micro-organisms were in some way involved in the primary oxidation of Fe(II) to Fe(III) in BIF (Ehrenreich & Widdel, 1994; Konhauser *et al.*, 2002; Kappler *et al.*, 2005). Two possible roles for bacteria are envisioned. The first is based on the production of O_2 by cyanobacteria, or their predecessors. These photoautotrophs would have flourished when nutrients were available and passively induced the precipitation of ferric hydroxide through their metabolic activity and/or by sorbing aqueous Fe species to the anionic ligands exposed on their surfaces (Konhauser, 1998). Other bacteria may have played a more active role in Fe(II) oxidation.

Table 1 Average macroband composition (in wt%) of the Dales Gorge Member, Hamersley Group, Western Australia

	SiO_2	Al_2O_3	Fe_2O_3	MgO	CaO	Na_2O	K_2O	P_2O_5	MnO	S	LOI*
BIF-type	43.15	0.09	46.37	2.69	1.65	0.04	0.02	0.21	0.05	0.03	4.06
S-type	45.78	2.04	27.77	5.21	2.85	0.02	0.28	0.16	0.24	0.32	14.34

Analyses are based on core from Paraburdoo DDH 44. Note: LOI (loss on ignition) includes the loss of H_2O, CO_2, and S.
Data from Ewers and Morris (1981).

For instance, Holm (1989) speculated that oxidation of dissolved Fe(II) by chemolithoautotrophic bacteria (e.g. *Gallionella ferruginea*) would have been kinetically favoured in an ocean with limited free oxygen because abiological rates of Fe(II) oxidation at circumneutral pH are sluggish under microaerobic conditions (e.g. Liang *et al.*, 1993). Meanwhile, Hartman (1984) first suggested that anoxygenic photosynthetic bacteria may have coupled the C and Fe cycles prior to the evolution of oxygenic photosynthesis. Since then, a number of experimental studies have indeed confirmed that various purple and green phototrophic bacteria can use Fe(II) as a reductant for CO_2 fixation (e.g. Widdel *et al.*, 1993; Heising *et al.*, 1999; Straub *et al.*, 1999).

The biological story on BIF, however, tends to neglect what happens to the organic remains and ferric hydroxide particles as they settle through the water column and become deposited at the sea floor. Given that the bulk water column was anoxic, perhaps with the exception of an upper layer of oxygenated waters above the chemocline of a stratified ocean (e.g. Klein & Beukes, 1989), the ferric hydroxide would have represented a favourable electron acceptor for the oxidation of the cellular remains. Certainly, the capacity of extant hyperthermophilic *Bacteria* and *Archaea* (that branch deeply in the universal phylogenetic tree) to reduce Fe(III) (Vargas *et al.*, 1998), and the recent observations of highly negative $\delta^{56}Fe$ values in magnetite-rich BIF samples as old as 2.9 Ga (Johnson *et al.*, 2003; Yamaguchi *et al.*, 2005), with comparable negative fractionations as observed in experimental cultures with dissimilatory Fe(III)-reducing bacteria (e.g., Johnson *et al.*, 2005), point towards the antiquity of such an anaerobic respiratory pathway. Significantly, coupling the reduction of Fe(III) minerals to the oxidation of organic matter not only explains the low content of organic carbon in the BIFs (<0.5 wt%; Gole & Klein, 1981), but it also explains the abundance of light carbon isotopic signatures associated with the interlayered carbonate minerals (Perry *et al.*, 1973; Walker, 1984; Baur *et al.*, 1985).

In this work, we calculate the amount of microbial Fe(III) reduction that might have taken place on the sea floor at certain times during the deposition of major BIF deposits, such as the 2.5 billion-year-old Dales Gorge Member of the Brockman Iron Formation, Hamersley Group in Western Australia. We assume that during periods of rapid Fe deposition (with the ferric hydroxide originating through the activity of photoferrotrophs only), 1 mm of unconsolidated sediment was deposited annually throughout the depositional environment, perhaps as vast as 1×10^{11} m^2 (areal extent of the Hamersley range). The deposition rate is similar to that estimated by Barley *et al.* (1997) for unconsolidated BIF sediments, and within an order of magnitude of the compacted BIF sedimentation rate (0.033 mm year^{-1}) as proposed by Pickard (2002), based on SHRIMP (sensitive high-resolution ion microprobe) U-Pb ages of zircons in tuffaceous mudrocks of the Brockman IF. Using compaction estimates of 95% (Trendall & Blockley, 1970), the 0.033 mm year^{-1} translates into an unconsolidated deposition rate of 0.66 mm year^{-1}. Furthermore, based on a presumed initial deposit of 80% Fe(OH)$_3$ and 20% amorphous SiO_2 (which is now manifest as Fe-rich mesobands in oxide-type BIF containing approximately 80% haematite/magnetite and 20% quartz; Konhauser *et al.*, 2002), with corresponding densities of 3.8 g cm^{-3} and 2.2 g cm^{-3}, respectively, the annual mass of Fe deposited could have been as high as 26.2 mol m^{-2}. We are not concerned here with deposition of other oxide-type BIF mesobands (i.e. the 'varves') or the S-type macrobands (i.e. chert–carbonate–silicate layers).

THE DIAGENETIC MODEL

Depositional setting

It is generally believed that the thick, laterally extensive BIF deposits, such as in the Hamersley Group, formed on partially isolated, submerged platforms on the continental shelves of Archean cratons (Morris & Horwitz, 1983; Simonson & Hassler, 1996). Water depths were below wave base, but shallow enough for carbonate precipitation, while some form of physical barrier was inferred as a means of explaining the absence of terrigenous siliciclastic sediment coarser than clay size. Pulsed hydrothermal output from distal mid-ocean-ridge (MOR) settings or hotspots was the major source of iron (e.g. Jacobsen & Pimentel-Klose, 1988), possibly supplemented by normal continental drainage (e.g. Canfield, 1998). The hydrothermal waters were brought onto the outer continental shelf by upwelling currents (Klein & Beukes, 1989) or plumes (Isley, 1995), and minerals subsequently precipitated uniformly throughout much of the depositional basin, as made evident by the general pattern of mesoband correlation (Trendall & Blockley, 1970; Ewers & Morris, 1981). The BIF-type macrobands are interspersed with S-type macrobands that reflect sustained episodes of volcanic ash input (Morris, 1993). Within the BIF-type macrobands, the Fe-rich mesobands, consisting today predominantly of iron in the form of haematite and magnetite, formed during major episodes of

hydrothermal input that may have lasted a few years to a few decades at most. On the other hand, genesis of the silica-rich mesobands indicate either periods of relative hydrothermal quiescence or the temporary failure of hydrothermal fluids reaching the BIF depositional basin (i.e. current reorganization). The varved units may have formed during intermediate stages. In either case, the absence of Fe led to periods dominated by silicification or calcium carbonate precipitation (Morris, 1993; Hamade *et al.*, 2003).

An alternate view to the shelf model has been provided by Krapež *et al.* (2003) and Pickard *et al.* (2004). They suggest that the S-macrobands of the Brockman IF are mostly shelf-derived epiclastic and volcaniclastic mud-rich turbidites deposited as distal lowstand fans in a sediment-starved abyssal plain setting. The precursor sediments to the BIF-type macrobands formed instead as pelagic muds on the flanks of submarine volcanoes during sea level high stands, which were then re-sedimented by density currents towards the same deep marine depositional setting. Fluxes of Si-rich shelf and Fe-rich hydrothermal sediments were pulsed, with gaps in sedimentation being recorded by wide-scale sea floor silicification that produced the chert-rich components.

In both depositional models, it is implicit that Fe(II) oxidation and Fe(III) hydrolysis occurred within the euphotic zone, with ferric hydroxide and biomass settling through the water column to the sea floor. For our calculations, we assume (i) that the bulk of the Fe(II) component in Fe-rich BIF-type mesobands formed secondarily through biological Fe(III) reduction, i.e. the magnetite is not primary (see succeeding discussions), and the decomposition of siderite into magnetite was not a significant process during early diagenesis (Kaufman *et al.*, 1990), and (ii) that the primary ferric hydroxide formed over an area equivalent to modern outcrop exposure. We therefore adopt the more traditional continental shelf model, particularly because the deep-water model does not yet account for some other synchronous BIF deposits, such as the Kuruman Iron Formation, South Africa, where BIFs shoal upwards and are overlain by shallow stromatolitic carbonates and granular iron formations (Klein & Beukes, 1989). Quite possibly, there was oxidation of hydrothermal Fe(II) at and near the source, as well as in more distal shallow water settings, as proposed here (Mark Barley, pers. comm.).

Quantification of reducing equivalents for magnetite formation

There are a number of reduced iron phases in BIF (Table 2). Some are considered to represent primary precipitates that formed within the anoxic water column (e.g. spheroidal siderite), when concentrations of ferrous iron and bicarbonate, originating from a combination of hydrothermal sources and microbial respiration of sedimented organic carbon, exceeded siderite solubility (Beukes *et al.*, 1990; Tice & Lowe, 2004). Other ferrous iron minerals, including magnetite, rhombic siderite, ferrosilicates (stilpnomelane, chlorite), ankerite,

Table 2 Mineral composition of the Dales Gorge Member in Paraburdoo DDH 44

| BIF-type macrobands	S-type macrobands
Quartz	Quartz
Haematite	Siderite-ankerite
Magnetite	Chlorite
Siderite–Ankerite	Talc (Ferroan)
Talc (ferroan)	Stilpnomelane
Stilpnomelane	K feldspar
Riebeckite	Pyrite
Chlorite	Mica
Apatite	Apatite

Note: Minerals listed in approximate order of abundance.
Data from Ewers and Morris (1981).

and pyrite, formed during diagenesis and metamorphism (e.g. Ayers, 1972; Perry *et al.*, 1973; McConchie, 1987). In the BIF-type macrobands of the Brockman Iron Formation, magnetite is commonly the second most abundant mineral phase after quartz in the centre of the depositional basin, whereas haematite is more abundant at the margins, followed by magnetite. The Fe-carbonates and Fe-silicates are more important in S-type macrobands and non-BIF mudrocks, whereas pyrite is typically limited to either the black shales interlayered with BIF or the S-type macrobands, where sulphur accounts for less than 0.3 wt% (Ewers & Morris, 1981). In terms of magnetite, there are also corresponding textural variations, indicating high regional metamorphic grade at the centre of the basin, but never beyond lower greenschist facies (Kaufman *et al.*, 1990).
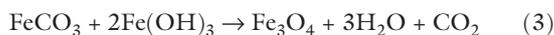
What fraction of the magnetite formed through bacterial Fe(III) reduction or as a by-product of the reaction of kerogenous carbon with ferric hydroxide or haematite during metamorphism is unresolved. Recent experimental studies have documented that magnetite can be formed in association with suspended cultures of phototrophic Fe(II)-oxidizing bacteria, through the reaction of Fe(II) with biogenic ferric hydroxide precipitates (Jiao *et al.*, 2005). These experiments were, however, conducted in 10 mM $FeCl_2$ solutions, and it will need to be assessed whether such a process can occur in fluids that better mimic the Archean oceans. Importantly, a number of petrographic studies have described the secondary origins of the magnetite in the Brockman BIF, conflicting with a direct chemical formation as described above (e.g. Han, 1978; McConchie, 1987; Morris, 1993). Indeed, Krapež *et al.* (2003) report several forms of diagenetic magnetite, including (i) disseminated grains within but obscuring sedimentary laminae (2) laminated beds that clearly truncate sedimentary layering, (3) layer-discordant veins, and (4) cleavage fills. Ewers & Morris (1981) report that most magnetite overgrew fine-grained haematite.

Based on cores from Paraburdoo, a site located in the south-west edge of the Hamersley range, it has been estimated that at least a quarter to a third of the iron now in the Dales Gorge Member was converted to magnetite, whereas the rest is

haematite (Morris, 1993). This makes the total amount of iron incorporated in magnetite as high as 8.7 mol m^{-2} (1/3 of 26.2 mol m^{-2}, the total estimated amount of ferric hydroxide deposited annually). During Fe(III) reduction, a 1C:4Fe(III) ratio is required if organic carbon – here assumed to be acetate with an average carbon oxidation state of 0 – serves as the reductant for chemoheterotrophic metabolism [reaction 1].

$$CH_3COO^- + 8Fe(OH)_3 \rightarrow$$
$$8Fe^{2+} + 2HCO_3^- + 15OH^- + 5H_2O \quad (1)$$
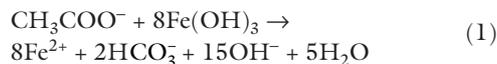
Fe$_3$O$_4$ has 1/3 Fe(II) and 2/3 Fe(III) (see reaction 2), which means that of the 8.7 mol Fe m^{-2} in magnetite, only 2.9 mol m^{-2} of Fe(II) came from Fe(III) reduction. In other words, 1/9 of the Fe-rich mesobands is Fe(II), whereas the other 8/9 remains Fe(III). Correspondingly, only 0.7 mol m^{-2} of buried C were required to form magnetite, i.e. a 1C:36Fe(III) ratio. The amount of organic carbon required would have been even less if some magnetite formed via a siderite precursor (reaction 3).

$$8Fe^{2+} + 16Fe(OH)_3 + 16OH^- \rightarrow 8Fe_3O_4 + 32H_2O \quad (2)$$

$$FeCO_3 + 2Fe(OH)_3 \rightarrow Fe_3O_4 + 3H_2O + CO_2 \quad (3)$$

It should be noted, however, that these Fe-rich mesobands are not representative of the entire BIF, which includes the ferrous iron minerals comprising the S-macrobands and the varved mesobands in the BIF-type macrobands. For example, some mesobands consist entirely of diagenetic siderite (reaction 4). Under those circumstances (complete Fe(III) reduction to Fe(II)), with 26.2 mol Fe m^{-2} deposited, some 6.6 mol m^{-2} of C were required as reductants, thereby maintaining the 1C:4Fe(III).

$$8Fe^{2+} + 16HCO_3^- \rightarrow 8FeCO_3 + 8H_2O + 8CO_2 \quad (4)$$

Given that BIFs are an assemblage of different iron minerals, it is not surprising that the average overall oxidation state of BIF is Fe$^{2.4+}$ (Klein & Beukes, 1992).

Biological oxidation of Fe(II) and BIF deposition

Konhauser *et al.* (2002) proposed that biological oxidation could have accounted for all of the ferric iron incorporated in BIF, with cell densities of Fe(II)-oxidizing bacteria considerably less than those found in most modern Fe-rich aqueous environments. Recently, Kappler *et al.* (2005) have calculated that a 17.6 m-thick layer of phototrophic Fe(II)-oxidizing bacteria, *Rhodobacter ferrooxidans* strain SW2, growing at a depth of at least 100 m below the wind-mixed surface layer of the ocean, and oxidizing Fe(II) at a rate of 0.014 mM day^{-1} (under ideal nutrient conditions), throughout an area equivalent to the present outcrop area in the Hamersley (1×10^{11} m^2), could generate 9.0×10^{12} mol

Fe(III) annually, or an amount equivalent to 90.0 mol Fe(III) m^{-2} year^{-1}. This rate is over three times as high as needed to explain the estimated amount of ferric iron deposited annually in the Dales Gorge Member depositional environment (recall 26.2 mol Fe m^{-2}), yet it is still less than the estimated amount of dissolved Fe in the 'basin' water column (2.0×10^{13} mol), based on a concentration of 0.5 mM (Morris, 1993) spread over 1×10^{11} m^2, with a mean water column depth of 400 meters (i.e. between sea floor and photosynthetic microbial community). This could have yielded a residence time for dissolved Fe(II) of 2 years, which corresponds to fast modern coastal upwelling rates of 0.5 m day^{-1} (Broecker & Peng, 1982).

Of course, the actual amount of Fe(II) oxidized in a late Archean ocean is unknown, so the total amount of Fe(III) determined by Kappler *et al.* (2005) must be viewed as a rough, but first attempt at predicting the Fe(II) oxidizing potential of a population of anoxygenic phototrophic bacteria that might have existed in the water column under nutrient sufficient conditions. Those calculations also have to be tempered against a phosphate crisis proposed to have existed at that time because of phosphate adsorption onto sedimenting ferric hydroxide particles, which would have led to diminished photosynthetic activity (Bjerrum & Canfield, 2002), and hence, reduced the amount of Fe(III) biologically generated. Furthermore, upwelling rates may have been slower, thereby limiting the amount of available Fe(II), or dissolved Fe(II) concentrations in the basin may actually have been similar to bulk ocean waters (0.05 mM) that were in equilibrium with the solubility of siderite and calcite (Holland, 1984). Nevertheless, we have purposefully tried to be conservative with our assumptions of Fe(III) production. First, Kappler *et al.* (2005) measured Fe(II) oxidation rates for strain SW2 at light intensities well below saturation (150 lux or approximately 3 μmol quanta m^{-2} s^{-1}) and at a narrow light wavelength range (<650 nm) that did not allow the cells to utilize their primary bacteriochlorophyll pigments. Second, they demonstrated that other anoxygenic bacteria (*Thiodictyon* sp. strain F4) could oxidize Fe(II) at rates much higher than *R. ferrooxidans* strain SW2. Consequently, the total mass of ferric hydroxide formed could have been substantially higher if the supply of Fe(II), or nutrients, to support the microbial community, were available.

Fate of photoautotroph biomass

In cultures of Fe(II)-oxidizing photoautotrophic bacteria, metabolism theoretically yields a molar ratio of 4Fe:1C (reaction 5). If cells growing at 150 lux generate Fe(III) at the rate of 90.0 mol m^{-2} year^{-1}, then the carbon produced annually is $\frac{1}{4}$, that is 22.5 mol m^{-2}, or 2.3×10^{12} mol for the Hamersley depositional environment. To put this number into context, using numbers from Canfield (2005), total net primary productivity in the late Archean-Palaeoproterozoic oceans is estimated at $(1.8–5.6) \times 10^{14}$ mol C year^{-1}, whereas Kharecha *et al.* (2005) have calculated that photoferrotrophs

alone could have produced up to 1.9×10^{13} mol C year^{-1} (throughout all oceans) by utilizing Fe(II) upwelled at a rate of 4 m year^{-1}.

$$4Fe^{2+} + CO_2 + 11H_2O \rightarrow CH_2O + 4Fe(OH)_3 + 8H^+ \quad (5)$$

However, when the amount of Fe(III) produced in the euphotic zone is compared with the amount incorporated into the BIF, at least 70% of the ferric hydroxide could have been recycled back into the water column (26.2 mol m^{-2} year^{-1} compared to 90.0 mol m^{-2} year^{-1}). That means at a 4Fe:1C reductive ratio, 15.9 mol C m^{-2} must have been used in reducing the excess Fe(III) precipitated by strain SW2 (63.8 mol m^{-2}) before burial. Importantly, from the 22.5 mol C m^{-2} that we hypothesize were sedimented along with the ferric hydroxide particles from the euphotic zone, 5.9 mol C m^{-2} remains unaccounted for after magnetite formation, and thus represent that fraction either oxidized by metabolic processes other than Fe(III) reduction or that lost to the water column. By comparison, assuming 100% of the Fe in BIF is in the form of siderite, then no additional metabolic processes are required.

If the bulk of the Fe(III) formed was recycled, where then did the reduction occur; in the water column, at the sediment–water interface or within the sediment column? To even begin addressing this point, we first need to compare the particle deposition rate to the Fe(III) reduction rate. In the first instance, electron micrographs show that the phototrophic Fe(II)-oxidizing bacteria are intimately associated with the ferric hydroxide particles (Kappler & Newman, 2004), and confocal laser microscopy images show that the particles themselves form quasi-spheres about 30 μm in diameter, to which more bacteria are attached on the outer surfaces (Fig. 1; unpublished images from Kappler & Newman, 2004). Based on the spherical morphology of the aggregate, we invoke the Stokes Law to calculate the particle deposition rate (equation 6).

$$v = (2gr^2)(\rho_p - \rho_w)/9\mu \quad (6)$$

where v is velocity (cm s^{-1}); g is gravity (981 cm s^{-2}); r is radius of aggregate (cm); ρ_p is density of particle (g cm^{-3}); ρ_w is density of sea water (g cm^{-3}); and μ is the viscosity of sea water (g cm^{-1} s^{-1}). The average particle radius is 15 μm; the density of primary ferric hydroxide precipitate is 1.9 g cm^{-3} (the actual density is 3.8 g cm^{-3}, but we assume the material is highly porous: we also neglect the density of the bacteria themselves attached to the iron particles because they are orders of magnitude less dense); the density of sea water at 30 °C is 1.022 g cm^{-3}; and the viscosity of sea water at 30 °C is 8.15×10^{-3} g cm^{-1} s^{-1} (Jumars *et al.*, 1993). This gives an estimated particle settling rate of 0.05 cm s^{-1}. Assuming that the BIF depositional environment had an average mean depth of 500 m (Trendall, 2002), then the particles formed at depth of 100 m (the euphotic zone) would have taken roughly 9 days to travel the 400 m to reach the sea floor. Furthermore,
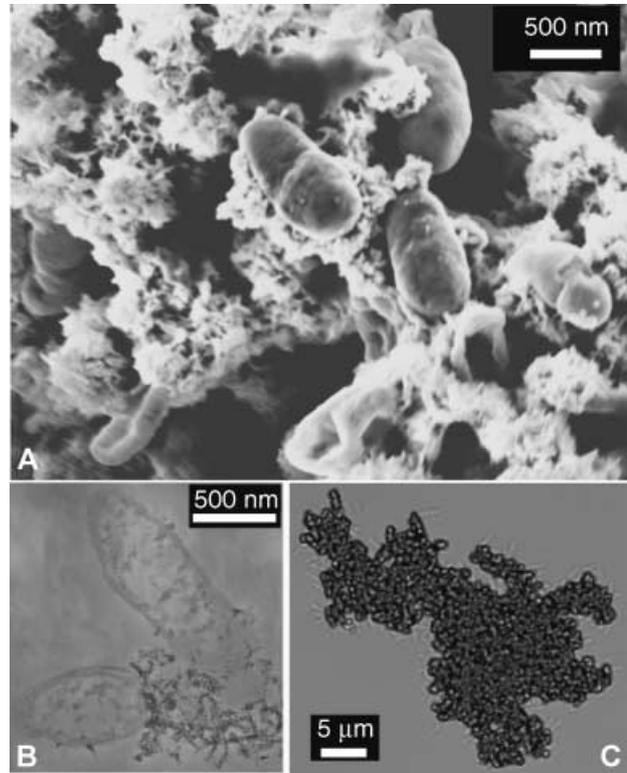

Fig. 1 Representative scanning (A) and transmission (B) electron micrographs, and (C) a confocal microscope image showing bacteria–mineral aggregates consisting of phototrophic Fe(II)-oxidizing *R. ferrooxidans* strain SW2 cells attached to the ferric hydroxide particles. Statistical analysis (not shown) indicated an average particle diameter of ~30 μm. For methodology on obtaining images, see Kappler & Newman (2004).

considering the 90.0 mol m^{-2} of ferric hydroxide precipitated each year (or 9.6×10^3 g m^{-2}, based on a molar mass of 107 g), divided by the density of ferric hydroxide, gives an approximate thickness up to 5 mm. The latter value is comparable to some rapidly accreting modern marginal marine settings (Henrichs & Reeburgh, 1987), and corresponds to our predicted accumulation rate of 1 mm year^{-1} ferric hydroxide/amorphous silica sediment.

Experimental rates of Fe(III) reduction for populations of various Fe(III)-reducing bacteria (e.g. *Geobacter metallireducens, Shewanella putrefaciens, Shewanella alga*), using fermentation products (e.g. H_2, lactate and acetate) as the electron donors, average 2.2×10^{-3} mol (or 0.12 g) Fe(III) g^{-1} Fe(OH)$_3$ day^{-1}, with a surface area of 600 m^2 g^{-1} (see Roden, 2003 for compilation). Assuming that the bulk of Fe(III) reduction took place at the sea floor (the fast settling rates of 0.05 cm s^{-1} means that a particle travels through 1L volume –10 cm path length – in 3 min), then the annual mass of ferric hydroxide deposited, divided by the Fe(III) reduction rate calculated previously, indicates that it might have taken a population of Fe(III) reducers (averaging 10^8–10^9 cells mL^{-1}) only a few days to reduce all of the available solid-phase Fe(III).

## IMPLICATIONS OF THE MODEL

Excess Fe(III) in the sediments

One of the most intriguing questions regarding a microbial role in the deposition of Precambrian BIF is the fate of the electrons temporarily fixed in the form of organic biomass. The attachment of Fe(II)-oxidizing cells to the iron minerals will lead to the deposition of cell biomass onto the sea floor. If this process were quantitative, then all Fe(III) would be re-reduced using the electrons associated with the biomass, and no solid-phase iron would have remained to later dehydrate into haematite or transform into magnetite. From the presence of those minerals in the BIF-type macrobands, however, we assume that the Fe(III):C_{org} ratio in the deposited material exceeded 4 : 1. In fact, we calculate that only 3% of the carbon initially generated (0.7 mol C m^{-2} of 22.5 mol C m^{-2}) was buried into the bottom sediments, along with primary Fe(OH)$_3$, to be used in magnetite formation during diagenesis and metamorphism: even less would have been required if some magnetite formed via a primary siderite precursor (Kaufman *et al.*, 1990). Additionally, once magnetite forms, the Fe(III) in it is not readily reducible by micro-organisms because magnetite is thermodynamically stable under a wide range of environmental conditions. So far, only two *Shewanella* species have been shown capable of using magnetite as an electron acceptor in their metabolism, thus reducing and dissolving magnetite (Kostka & Nealson, 1995). Fe(III) reduction is also strongly dependant on available mineral surface area (Roden, 2003), and the transformation of ferric hydroxide to magnetite decreases the surface area from approximately 600 m^2 g^{-1} to 4.0–6.6 m^2 g^{-1}, respectively (Cornell & Schwertmann, 2003), resulting in lower overall Fe(III) reduction rates.

The change in Fe:C ratio during magnetite formation, leading to the excess of Fe(III) in the sediments, could have come about in one of five ways: via (i) chemolithoautotrophic O_2^- dependent Fe(II) oxidation precipitating more Fe(III); (ii) nonquantitative cell-mineral aggregation during photoautotrophic Fe(II) oxidation; (iii) density current segregation of carbon and Fe(III), (iv) preferential mobilization of fermentation products relative to Fe(III), and/or (v) loss of carbon to another anaerobic respiratory process, limiting Fe(III) reduction. These five ways are described below:

(1) There may have been more ferric hydroxide produced in the euphotic zone relative to carbon fixed as biomass, thus increasing the Fe:C ratio in excess of 4 : 1. In Kappler *et al.* (2005), we showed that a 17.6 m layer of anoxygenic phototrophs could have oxidized all Fe(II) before it reached an overlying layer of cyanobacteria. Therefore, in that model, all ferric hydroxide was generated photoautotrophically under anoxic conditions. Nonetheless, it is also possible that chemolithoautotrophic bacteria, such as the microaerophilic *Gallionella ferruginea*, may have coexisted with the photoferrotrophs. The former might have oxidized a fraction of

dissolved Fe(II) that diffused upwards through the layer of anoxygenic phototrophs above the chemocline, using O_2 as the electron acceptor (reaction 7). If this 'additional' ferric hydroxide also sank to the sea floor, then the combined metabolisms would have changed the Fe:C ratio in favour of more ferric Fe (III) being deposited.

$$6Fe^{2+} + 0.5O_2 + CO_2 + 16H_2O \rightarrow$$
$$CH_2O + 6Fe(OH)_3 + 12H^+ \quad (7)$$
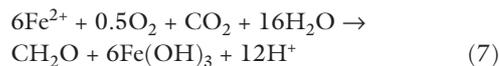
(2) If anoxygenic photosynthetic bacteria solely generated all of the Fe(III), then excess Fe(III) in the sediments could have occurred if there was a nonquantitative association of cells with the ferric hydroxide. For instance, experiments with the photosynthetically Fe(II)-oxidizing strain SW2 have shown that the percentage of planktonic cells remaining in suspension after Fe(II) oxidation, relative to the total number of cells produced, ranges from 33% to only 1%, with a higher number of planktonic cells occurring when the cultures were inoculated with a lower numbers of cells (Fig. 2; unpublished data from Kappler *et al.*, 2005). Given that a substantial amount of cells can be maintained in the water column, when those cells lysed, diffusive distribution of organic matter into upper layers of the water column may have facilitated aerobic respiration, whereas the ferric hydroxide instead sank to the sea floor.

(3) If the S-macroband components were resuspended from the shelf to the abyssal plain via density currents (Krapež *et al.*, 2003; Pickard *et al.*, 2004), then it is possible that similar physical processes acted on the Fe-rich precursor sediments (that we suggest formed on the shelf as well), leading in some way to the segregation of the Fe(III) and organic components.

(4) During deposition and accumulation at the sea floor, some biomass would have been converted through fermentation and hydrolysis into simpler compounds, such as dissolved organic carbon (DOC; amino acids and short-chain fatty acids, such as lactate and acetate) and H$_2$. A fraction of the fermentation products could have diffused away from the immediate environment, relative to the immobile ferric hydroxide, thereby removing electrons that otherwise would have been available to reduce Fe(III). Crucially, if the DOC was redistributed to, and incorporated into, sediment deficient in ferric hydroxide that accumulated beneath biologically unproductive waters, then it would ultimately have been tied to another form of microbial respiration; see point 5 (Walker, 1984).

(5) Despite the probability of a surface water oxic zone generated by cyanobacterial activity (Summons *et al.*, 1999), deep waters remained anoxic (e.g. Canfield, 1998). In the absence of O_2, the fermentation products in the bottom waters and/or shallow sediments (from point #4) would have been oxidized via some other form of anaerobic respiratory process (Rothman *et al.*, 2003). In terms of such pathways, the paucity of O_2 would have meant minimal nitrate and sulphate availability; the latter being evident from negligible sulphur isotopic fractionations between late Archean-early Palaeoproterozoic
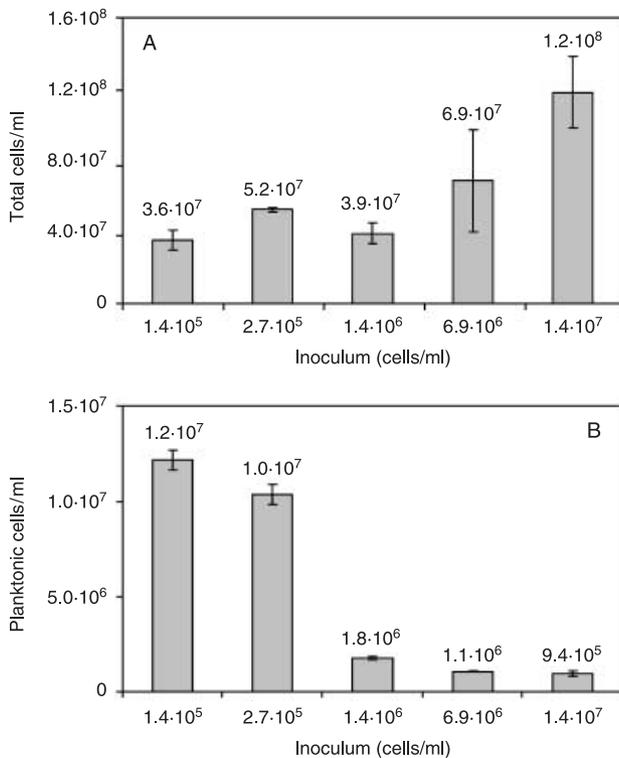
Fig. 2 Cell numbers in cultures of *R. ferrooxidans* strain SW2 oxidizing Fe(II) at different initial cell inoculations. (A) Total number of cells in cultures and (B) number of planktonic cells (not-mineral attached, and thus not settled to the bottom of the bottle). Note the different scale in the graphs. For methodology on growing the cells, see Kappler *et al.* (2005). Cells in Fe-mineral containing culture suspensions were counted from cultures incubated upside down. The sides of the bottles were covered with aluminium foil so the light could penetrate the bottles only from the top (flat glass) to simulate growth in a light-penetrated water column. Total number of cells were counted after vigorous shaking to homogenize the cultures that consisted of free cells, settled minerals and cell-mineral aggregates. First, 1 mL of the suspension was fixed with 0.1 mL of 25% gluteraldehyde. An 8.9-mL solution, with 28 g of ammonium oxalate, 15 g of oxalic acid per litre and 1 mL of an anoxic solution of ferrous ethylenediammonium sulphate (100 m$_M$), were then added. The vials were then swirled periodically for 10 min until all of the Fe-mineral particles had dissolved. A volume of 0.1–1 mL was filtered onto a black Nucleopore® polycarbonate filter (Whatman, Clifton, NJ, USA), and then stained with DAPI (4′,6-diamidino-2-phenylindole, final concentration of approximately 5 μg mL^{-1}). The cells present within a certain field of view were counted using the computer software METAMORPH (Universal Imaging Corporation, Downington, Pennsylvania), connected to a fluorescence microscope (Axioplan, Zeiss, Germany). Free-floating (planktonic) cells present in the culture supernatant were counted using the same protocol, but by withdrawing liquid from the supernatant through the rubber stopper with a syringe equipped with a long needle to avoid re-suspending the settled Fe(III)-mineral precipitates.

sulphide and sulphate minerals (Strauss, 2003), and the absence of pyrite in BIF, except in association with interlayered shaley units (Ewers & Morris, 1981). The supply of MnO_2 was also likely not very significant given that the concentration of Mn(II) released in hydrothermal effluent is up to five times lower than that of Fe (II) (Campbell *et al.*, 1988) and because

there are presently no known oxygen- or nitrate-independent Mn(II)-oxidizing bacteria. In contrast, there is evidence in favour of significant methanogenic activity at that time, i.e. coupling the oxidation of acetate or H_2 to methane formation. These include the kerogens from between 2.8 and 2.6 Ga with highly negative $\delta^{13}C$ signatures (between –40‰ and –60‰) that possibly formed as the result of methanogenic ^{12}C-rich gas production, the incorporation of this methane into the biomass of methanotrophic bacteria, and inevitably the preservation of ^{12}C-enriched organic matter (Hayes, 1983).

Role of methanogenesis for the loss of reducing equivalents

If methanogenesis was important, were the methanogens (i) geographically segregated from regions of Fe(III) reduction (i.e. not just vertically as in modern sediments) or (ii) in coexistence and competition with Fe(III) reducers for the fermentation products in the same sediments? In the first instance, it is quite probable that the two microbial communities were spatially separated from one another over much of the sea floor, with Fe(III) reduction occurring in sediments beneath highly productive waters, whereas methanogens dominated other sediments, using DOC transported away from sites of high productivity. However, despite observations in modern sediments that methane is not produced until the reducible Fe(III) fraction has been converted to ferrous iron (Lovley & Phillips, 1987), methanogenesis may have prevailed in competition if conditions for the Fe(III) reducers were made less favourable. This could have come about in two ways:

(1) Based on our calculations, the very rapid rates of sediment particle accretion would have led to exceptionally fast burial rates that effectively insulated the biomass-ferric hydroxide aggregates. Once buried, and no longer subject to mixing, the rates of Fe(III) reduction may have dropped markedly, as Fe(III) reduction is known to strongly depend on available mineral surface area (Roden, 2003). The apparent absence of sediment re-working by physical processes (as suggested in the well-defined and laterally continuous microbanding in varved mesobands), certainly implies that once buried, the ferric hydroxide sediment were not significantly re-mobilized.

(2) The availability of surface sites for Fe(III) reduction might also have been reduced by covering ferric hydroxide particles with solid-phase products of microbial Fe(III) reduction, such as magnetite (Lovley, 1990); by reacting with dissolved silica during particle descent [reaction 8] (Davis *et al.*, 2002); or by adsorption of Fe(II) to ferric hydroxide, leading to goethite formation (Roden & Urrutia, 2002).

$$2Si(OH)_4 + \,>FeOH^0 \rightarrow$$
$$>FeSi_2O_3(OH)_4^- + 2H_2O + H^+ \qquad (8)$$
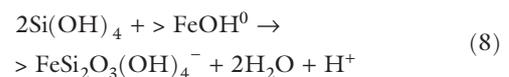
In the absence of silica-precipitating protists, the concentration of silica in the Precambrian oceans may have hovered at the

saturation state of amorphous silica, around 110 mg l^{-1} at 25 °C (Siever, 1992). This view is also supported by textural evidence of cherts in Palaeoproterozoic BIFs that suggest direct silica precipitation in subtidal settings, at or just below the sea floor (Pickard *et al.*, 2004; Maliva *et al.*, 2005). In an ocean water column, where there was a high concentration of descending ferric hydroxide particles (as we propose here), it is very likely that a significant concentration of silica would have been adsorbed, leading to the formation of amorphous ferric silicate phases (Siever & Woodford, 1973; Drever, 1974). Actually, experimental studies have documented that the presence of Fe(OH)$_3$ can remove so much silica that the resultant minerals contain up to 60% by weight SiO$_2$ (Harder & Flehmig, 1970). Agglomeration of the iron-silica particles, accentuating density differences, might have led to some segregation within the water column itself, but much of the coprecipitated silica could presumably have been entrained with the settling iron particles, and it was only during burial re-crystallization that the two components would have been dissociated, at times leading to the fine, but somewhat irregular microbanding (Morris, 1993). Significantly, the adsorption of silica to ferric hydroxide particles at the sea floor may have diminished the efficiency of the Fe(III)-reducing bacteria, a suggestion supported by recent studies on a sandy aquifer that showed the depletion of ferric hydroxide but not the ferruginous phyllosilicate fraction (Shelobolina *et al.*, 2004).

Ferric hydroxide can also be transformed to goethite by Fe(II)-catalysed (chemical) transformation within a matter of a few days (Hansel *et al.*, 2003). This transformation has even been shown to occur during phototrophic Fe(II) oxidation (Kappler & Newman, 2004). Such reactions are important because the rate of reduction for goethite is much lower than reduction of ferric hydroxide because of its lower surface area. For example, reduction of 50 mM goethite ceases when approimately 1.5 mM Fe(II) accumulates (Roden & Urrutia, 1999). This means that in the case of a Fe-rich Precambrian surface sediment, it is reasonable to assume that there may have been at least a significant slowdown of the rate of Fe(III) reduction. As a result, the unusual high cell numbers used in typical Fe(III) reduction experiments (e.g. 10^7–10^9 cells per millilitre) probably would not have been supported on the late Archean sea floor.

Ascribing a dominant role to methanogens, however, has to reconcile the carbon isotopic values of carbonate phases (siderite, ankerite, ferroan dolomite) interlayered with BIF. They tend to have δ^{13}C compositions averaging between −5‰ to −15‰ (e.g. Becker & Clayton, 1972; Baur *et al.*, 1985), values that are difficult to explain by methanogenic activity on the sea floor and their isotopically depleted CH$_4$ diffusing back into the water column, leaving behind the 'heavier' carbon fraction to be incorporated into the carbonates. It has been argued that much of the isotopically light carbon in the carbonates might have come from oxidation of organic carbon coupled to Fe(III) reduction (e.g. Walker, 1984), but perhaps, some

isotopically light methane was consumed *in situ* by methanotrophs that used Fe(III) as an electron acceptor? At present such micro-organisms have not yet been described, but thermodynamic considerations show that a coupling of CH$_4$ oxidation to Fe(III) reduction theoretically should be possible [reaction 9]. Although authigenic carbonates that form from the oxidation of methane coupled to sulphate reduction (i.e. at methane seeps) are typified by negative δ^{13}C values (as low as −60‰), less negative δ^{13}C values have been reported from carbonates when diluted with residual bicarbonate from the inorganic carbon pool utilized by the methanogens (Peckman & Thiel, 2004).

$$CH_4 + 8Fe(OH)_3 \rightarrow 8Fe^{2+} + CO_2 + 16OH^- + 6H_2O (\Delta G° \text{ at pH } 7 = -311 \text{ kJ})$$ (9)
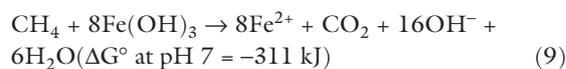
Residual organic matter burial

Given the potential presence of a mixed consortium of fermenters, Fe(III) reducers and methanogens at the sea floor, why then was some organic carbon even buried into the sediment to be oxidized during magnetite formation at a later stage? Perhaps, some of the carbon was entrained and sheltered within ferric iron particles after sedimentation by particle aggregation and compaction, and thus was not available to heterotrophic communities in the shallow sediment? Besides this physical protection, some carbon would also have been more refractory by its chemical composition, and not reduced until metamorphism at a later stage. Although biopolymers such as nucleic acids, proteins and carbohydrates are easily degraded and oxidized, fatty acids (e.g. phospholipids in membranes) and other more hydrophobic cell components (e.g. hopanes) are much more recalcitrant and can persist several hundreds of millions, or even billions, of years (e.g. Brocks *et al.*, 1999).

The carbon buried may also have arisen from the lysed cells of sediment microbial communities. Yet, the fermenters, Fe(III) reducers and methanogens would ultimately have utilized carbon from the lysed phototroph biomass, i.e. they grew heterotrophically. Furthermore, the growth yields of these processes was likely relatively poor compared to the phototrophs, thus a limited amount of biomass would actually have been generated by these metabolisms. Similarly, the reducing equivalents (as H$_2$) needed to fix the CO$_2$ for chemolithoautotrophic growth by Fe(III) reducers and methanogens would have been derived from the fermentative degradation of the phototrophic biomass. Only if an additional flux of reductant was available, e.g. hydrothermal H$_2$, would additional biomass have been created. That possibility, however, is not very probable if the BIFs formed on continental shelves, far removed from hot spot or mid-ocean ridge systems. Interestingly, in the absence of bottom water O$_2$, nitrate or sulphate, the most plausible pathway to generate biomass in the bottom sediments, aside from the settled phototrophic
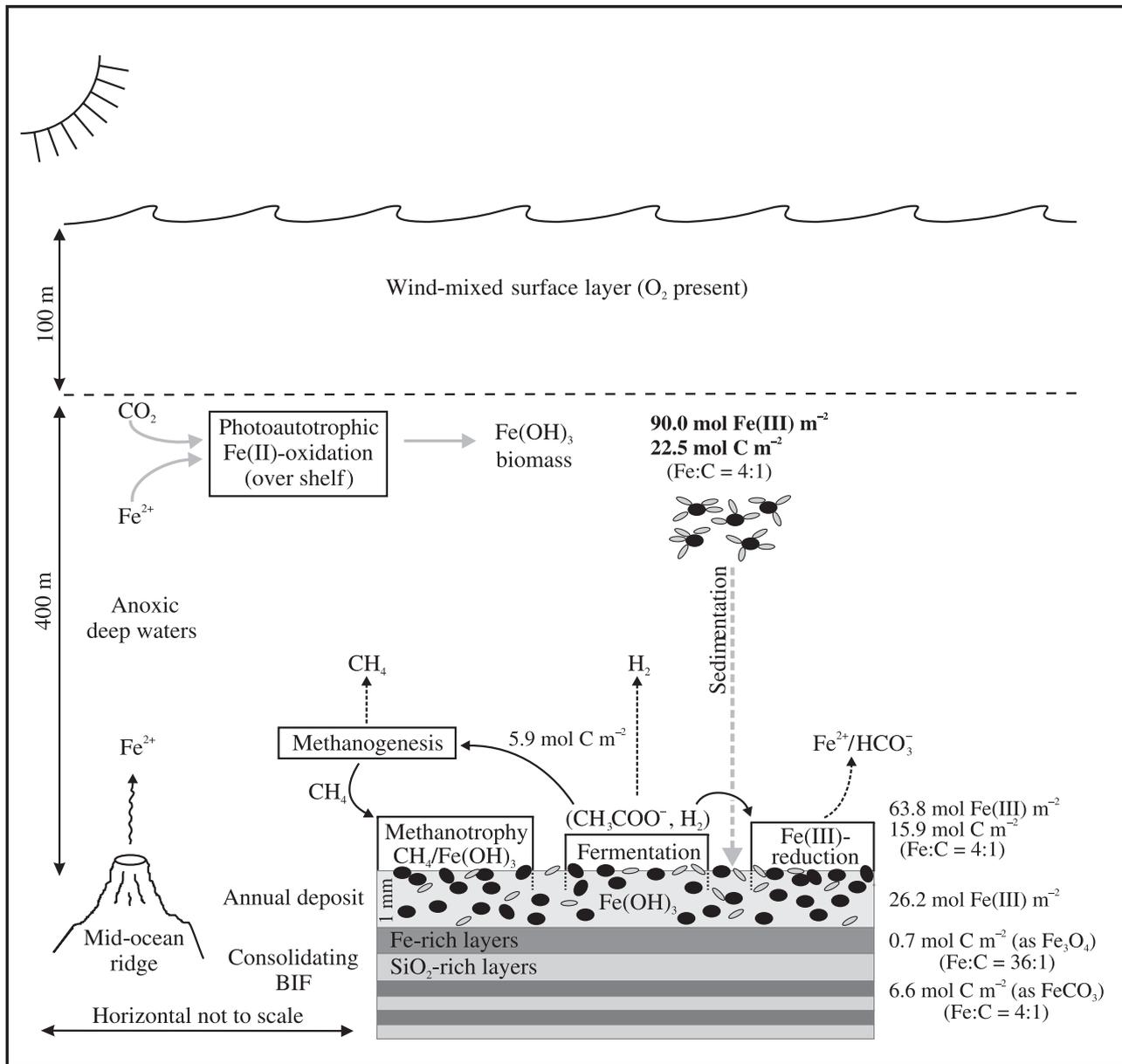
Fig. 3 Model for the biological role in Fe cycling in late Archean–Palaeoproterozoic oceans.

plankton, is through coupling methane oxidation to Fe(III) reduction.

CONCLUSIONS

Unlike the stratified water bodies with sulfidic bottom waters (e.g. Black Sea, Cariaco Trench) that have provided valuable insights into what chemical and microbiological processes might have taken place in the water column and sediments of the Mesoproterozoic to Neoproterozoic oceans, there are very few modern analogues for the anoxic, Fe-rich oceans of the late Archean and Palaeoproterozoic. Moreover, the BIFs

themselves have undergone post-depositional alteration, which makes any interpretation of their initial depositional history fraught with uncertainty. It is in this context that we have tried to provide a simple model that examines the relationship between photoautotrophic Fe(II) oxidation in the water column with metabolically driven redox reactions in the bottom sediments, driven by an active community of fermenters and Fe(III) reducers, and possibly methanogens and methanotrophs (Fig. 3). It has, however, also led to a number of unresolved questions regarding where was the bulk of the Fe(III) reduced, at what rates, and which micro-organisms were responsible for oxidizing the planktonic biomass?

ACKNOWLEDGEMENTS

REFERENCES

Ayers DE (1972) Genesis of iron-bearing minerals in banded iron formation mesobands in the Dales Gorge Member, Hamersley Group, Western Australia. *Economic Geology* **67**, 1214–1233.

Barley ME, Pickard AL, Sylvester PJ (1997) Emplacement of a large igneous province as a possible cause of banded iron formation 2.45 billion years ago. *Nature* **385**, 55–58.

Baur ME, Hayes JM, Studley SA, Walter MR (1985) Millimeter-scale variations of stable isotope abundances in carbonates from banded iron-formations in the Hamersley Group of Western Australia. *Economic Geology* **80**, 270–282.

Becker RH, Clayton RN (1972) Carbon isotopic evidence for the origin of a banded iron-formation in Western Australia. *Geochimica et Cosmochimica Acta* **36**, 577–595.

Beukes NJ, Klein C, Kaufman AJ, Hayes JM (1990) Carbonate petrography, kerogen distribution, and carbon and oxygen isotope variations in an early Proterozoic transition from limestone to iron-formation deposition, Transvaal Supergroup, South Africa. *Economic Geology* **85**, 663–690.

Bjerrum CJ, Canfield DE (2002) Ocean productivity before about 1.9 Gyr limited by phosphorous adsorption onto iron oxides. *Nature* **417**, 159–162.

Brocks JJ, Logan GA, Buick R, Summons RE (1999) Archean molecular fossils and early rise of eukaryotes. *Science* **285**, 1033–1036.

Broecker WS, Peng TH (1982) *Tracers in the Sea*. Lamont-Doherty Geological Observatory, New York.

Campbell AC, Palmer MR, Klinkhammer GP, Bowers TS, Edmond JM, Lawrence JR, Casey JF, Thompson G, Humphris S, Rona P, Karson JA (1988) Chemistry of hot springs on the mid-Atlantic Ridge. *Nature* **335**, 514–519.

Canfield DE (1998) A new model for Proterozoic ocean chemistry. *Nature* **396**, 450–453.

Canfield DE (2005) The early history of atmospheric oxygen: Homage to Robert M. Garrels, *Annual Reviews in Earth and Planetary Sciences* **33**, 17.1–17.36.

Cornell RM, Schwertmann U (2003) *The Iron Oxides: Structure, Properties, Reactions, Occurrences and Uses*, 2nd edn. Wiley-VCH, Weinheim, Germany.

Davis CC, Chen H-W, Edwards M (2002) Modelling silica sorption to iron hydroxide. *Environmental Science and Technology* **36**, 582–587.

Drever JI (1974) Geochemical model for the origin of Precambrian banded iron formations. *Geological Society of America Bulletin* **85**, 1099–1106.

Ehrenreich A, Widdel F (1994) Anaerobic oxidation of ferrous iron by purple bacteria, a new type of phototrophic metabolism. *Applied and Environmental Microbiology* **60**, 4517–4526.

Ewers WE, Morris RC (1981) Studies of the Dales Gorge Member of the Brockman iron formation, Western Australia. *Economic Geology* **76**, 1929–1953.

Gole MJ, Klein C (1981) Banded iron-formations through much of Precambrian time. *Journal of Geology* **89**, 169–183.

Hamade T, Konhauser KO, Raiswell R, Morris RC, Goldsmith S (2003) Using Ge: Si ratios to decouple iron and silica fluxes in Precambrian banded iron formations. *Geology* **31**, 35–38.

Han T-M (1978) Microstructures of magnetite as guides to its origin in some Precambrian iron-formations. *FortschrItte der Mineralogie* **56**, 105–142.

Hansel CM, Benner SG, Neiss J, Dohnalkova A, Kukkadapu RK, Fendorf S (2003) Secondary mineralization pathways induced by dissimilatory iron reduction of ferrihydrite under advective flow. *Geochimica et Cosmochimica Acta* **67**, 2977–2992.

Harder H, Flehmig W (1970) Quartzsynthese bei tiefen Temperaturen. *Geochimica et Cosmochimica Acta* **34**, 295–305.

Hartman H (1984) The evolution of photosynthesis and microbial mats: A speculation on the banded iron formations. In *Microbial Mats: Stromatolites* (eds Cohen Y, Castenholz RW, Halvorson HO). Alan Liss Inc., New York, pp. 449–453.

Hayes JM (1983) Geochemical evidence bearing on the origin of aerobiosis, a speculative hypothesis. In *Earth's Earliest Biosphere, its Origin and Evolution* (ed. Schopf JW). Princeton University Press, Princeton, NJ, pp. 291–301.

Heising S, Richter L, Ludwig W, Schink B (1999) *Chlorobium ferrooxidans* sp. *nov.*, a phototrophic green sulfur bacterium that oxidizes ferrous iron in coculture with a '*Geospirillum*' sp. strain. *Archives of Microbiology* **172**, 116–124.

Henrichs SM, Reeburgh WS (1987) Anaerobic mineralization of marine sediment organic matter: Rates and the role of anaerobic processes in the oceanic carbon economy. *Geomicrobiology Journal* **5**, 191–237.

Holland HD (1984) *The Chemical Evolution of the Atmosphere and Oceans*. Princeton University Press, Princeton, New Jersey.

Holm NG (1989) The $^{13}C/^{12}C$ ratios of siderite and organic matter of a modern metalliferous hydrothermal sediment and their implications for banded iron formations. *Chemical Geology* **77**, 41–45.

Isley AE (1995) Hydrothermal plumes and the delivery of iron to banded iron formation. *Journal of Geology* **103**, 169–185.

Jacobsen SB, Pimentel-Klose MR (1988) An Nd isotopic study of the Hamersley and Michipicoten banded iron formations: The source of REE and Fe in Archean oceans. *Earth and Planetary Science Letters* **87**, 29–44.

Jiao Y, Kappler A, Croal LR, Newman DK (2005) Isolation and characterization of a genetically tractable photoautotrophic Fe(II)-oxidizing bacterium, *Rhodopseudomonas palustris* strain TIE-1. *Applied and Environmental Microbiology* **71**, 4487–4496.

Johnson CM, Beard BL, Beukes NJ, Klein C, O'Leary JM (2003) Ancient geochemical cycling in the Earth as inferred from Fe isotope studies of banded iron formations from the Transvaal craton. *Contributions to Mineralogy and Petrology* **144**, 523–547.

Johnson CM, Roden EE, Welch SA, Beard BL (2005) Experimental constraints on Fe isotope fractionation during magnetite and Fe carbonate formation coupled to dissimilatory hydrous ferric oxide reduction. *Geochimica et Cosmochimica Acta* **69**, 963–993.

Jumars PA, Deming JW, Hill PS, Karp-Boss L, Yager PL, Dade WB (1993) Physical constraints on marine osmotrophy in an optimal foraging context. *Marine Microbial Food Webs* **7**, 121–159.

Kappler A, Newman DK (2004) Formation of Fe(III)-minerals by Fe(II)-oxidizing photoautotrophic bacteria. *Geochimica Cosmochimica Acta* **68**, 1217–1226.

Kappler A, Pasquero C, Konhauser KO, Newman DK (2005) Deposition of banded iron formations by anoxygenic phototrophic Fe(II)-oxidizing bacteria. *Geology* **33**, 865–868.

Kaufman AJ, Hayes JM, Klein C (1990) Primary and diagenetic controls of isotopic compositions of iron-formation carbonates. *Geochimica et Cosmochimica Acta* **54**, 3461–3473.

Kharecha PA, Kasting JF, Siefert JL (2005) A coupled atmosphere-ecosystem model of the anaerobic Archean biosphere. *Geobiology* **3**, 53–76.

Klein C, Beukes NJ (1989) Geochemistry and sedimentology of a facies transition from limestone to iron-formation deposition in the early Proterozoic Transvaal supergroup, South Africa. *Economic Geology* **84**, 1733–1774.

Klein C, Beukes NJ (1992) Time distribution, stratigraphy, and sedimentologic setting, and geochemistry of Precambrian iron-formations. In *The Proterozoic Biosphere: a Multidisciplinary Study* (eds Schopf JW, Klein C). Cambridge University Press, Cambridge, pp. 139–146.

Konhauser KO (1998) Diversity of bacterial iron mineralization. *Earth-Science Reviews* **43**, 91–121.

Konhauser KO, Hamade T, Morris RC, Ferris FG, Southam G, Raiswell R, Canfield D (2002) Did bacteria form Precambrian banded iron formations? *Geology* **30**, 1079–1082.

Kostka JE, Nealson KH (1995) Dissolution and reduction of magnetite by bacteria. *Environmental Science and Technology* **29**, 2535–2540.

Krapež B, Barley ME, Pickard AL (2003) Hydrothermal and resedimented origins of the precursor sediments to banded iron formations: Sedimentological evidence from the early Palaeoproterozoic Brockman supersequence of Western Australia. *Sedimentology* **50**, 979–1011.

Liang L, McNabb JA, Paulk JM, Gu B, McCarthy JF (1993) Kinetics of Fe(II) oxygenation at low partial pressure of oxygen in the presence of natural organic matter. *Environmental Science and Technology* **27**, 1864–1870.

Lovley DR (1990) Magnetite formation during microbial dissimilatory iron reduction. In *Iron Biominerals* (eds Frankel RB, Blakemore RP). Plenum Press, New York, pp. 151–166.

Lovley DR, Phillips EJP (1987) Competitive mechanisms for inhibition of sulphate reduction and methane production in the zone of ferric iron reduction in sediments. *Applied and Environmental Microbiology* **53**, 2636–2641.

Maliva RG, Knoll AH, Simonson BM (2005) Secular change in the Precambrian silica cycle: Insights from chert petrology. *Geological Society of America Bulletin* **117**, 835–845.

McConchie D (1987) The geology and geochemistry of the Joffre and Whaleback shale members of the Brockman Iron Formation, Western Australia. In *Precambrian Iron-Formations* (eds Appel PWU, LaBerge GL). Theophrastus, Athens, pp. 541–597.

Morris RC (1993) Genetic modelling for banded iron-formation of the Hamersley Group, Pilbara Craton, Western Australia. *Precambrian Research* **60**, 243–286.

Morris RC, Horwitz RC (1983) The origin of the iron-formation–rich Hamersley group of Western Australia – deposition on a platform. *Precambrian Research* **21**, 273–297.

Peckman J, Thiel V (2004) Carbon cycling at ancient methane-seeps. *Chemical Geology* **205**, 443–467.

Perry EC Jr, Tan FC, Morey GB (1973) Geology and stable isotope geochemistry of the Biwabik Iron Formation, northern Minnesota. *Economic Geology* **68**, 1110–1125.

Pickard AL (2002) SHRIMP U-Pb zircon ages of tuffaceous mudrocks in the Brockman Iron Formation of the Hamersley Range, Western Australia. *Australian Journal of Earth Sciences* **49**, 491–507.

Pickard AL, Barley ME, Krapež B (2004) Deep-marine depositional setting of banded iron formation: Sedimentological evidence from interbedded clastic sedimentary rocks in early Paleoproterozoic Dales Gorge Member of Western Australia. *Sedimentary Geology* **170**, 37–62.

Roden EE (2003) Fe (III) oxide reactivity toward biological versus chemical reduction. *Environmental Science and Technology* **37**, 1319–1324.

Roden EE, Urrutia MM (1999) Ferrous iron removal promotes microbial reduction of crystalline iron (III) oxides. *Environmental Science and Technology* **33**, 1847–1853.

Roden EE, Urrutia MM (2002) Influence of biogenic Fe(II) on bacterial crystalline Fe(III) oxide reduction. *Geomicrobiology Journal* **19**, 209–251.

Rothman DH, Hayes JM, Summons RE (2003) Dynamics of the Neoproterozoic carbon cycle. *Proceedings of the National Academy of Sciences of the United States of America* **100**, 8124–8129.

Shelobolina ES, Anderson RT, Vodyanitskii YN, Sivtsov AV, Yuretich R, Lovley DR (2004) Importance of clay size minerals for Fe(III) respiration in a petroleum-contaminated aquifer. *Geobiology* **2**, 67–76.

Siever R (1992) The silica cycle in the Precambrian. *Geochimica et Cosmochimica Acta* **56**, 3265–3272.

Siever R, Woodford N (1973) Sorption of silica by clay minerals. *Geochimica et Cosmochimica Acta* **37**, 1851–1880.

Simonson BM, Hassler SW (1996) Was the deposition of large Precambrian iron formations linked to major marine transgressions? *Journal of Geology* **104**, 665–676.

Straub KL, Rainey FA, Widdel F (1999) *Rhodovulum iodosum* sp. nov. and *Rhodovulum robiginosum* sp. nov., two new marine phototrophic ferrous-iron-oxidizing purple bacteria. *International Journal for Systematic Bacteriology* **49**, 729–735.

Strauss H (2003) Sulphur isotopes and the early Archaean sulphur cycle. *Precambrian Research* **126**, 349–361.

Summons RE, Jahnke LL, Hope JM, Logan GA (1999) 2-Methylhopanoids as biomarkers for cyanobacterial oxygenic photosynthesis. *Nature* **400**, 554–557.

Tice MM, Lowe DR (2004) Photosynthetic microbial mats in the 3,416-Myr-old ocean. *Nature* **431**, 549–552.

Trendall AF (2002) The significance of iron-formation in the Precambrian stratigraphic record. *Special Publication from the International Association of Sedimentology* **33**, 33–66.

Trendall AF, Blockley JG (1970) The iron formations of the Precambrian Hamersley Group, Western Australia; with special reference to the associated crocidolite. *Western Australia Geological Survey Bulletin* **119**, 336.

Vargas M, Kashefi K, Blunt-Harris EL, Lovley DR (1998) Microbiological evidence for Fe(III) reduction on early Earth. *Nature* **395**, 65–67.

Walker JCG (1984) Suboxic diagenesis in banded iron formations. *Nature* **309**, 340–342.

Widdel F, Schnell S, Heising S, Ehrenreich A, Assmus B, Schink B (1993) Ferrous iron oxidation by anoxygenic phototrophic bacteria. *Nature* **362**, 834–836.

Yamaguchi KE, Johnson CM, Beard BL, Ohmoto H (2005) Biogeochemical cycling of iron in the Archean Paleoproterozoic Earth: Constraints from iron isotope variations in sedimentary rocks from the Kaapvaal and Pilbara Cratons. *Chemical Geology* **218**, 135–169.